eLIFE
elifesciences.org

Figures and figure supplements

The Notch-mediated hyperplasia circuitry in *Drosophila* reveals a Src-JNK signaling axis

Diana M Ho, et al.

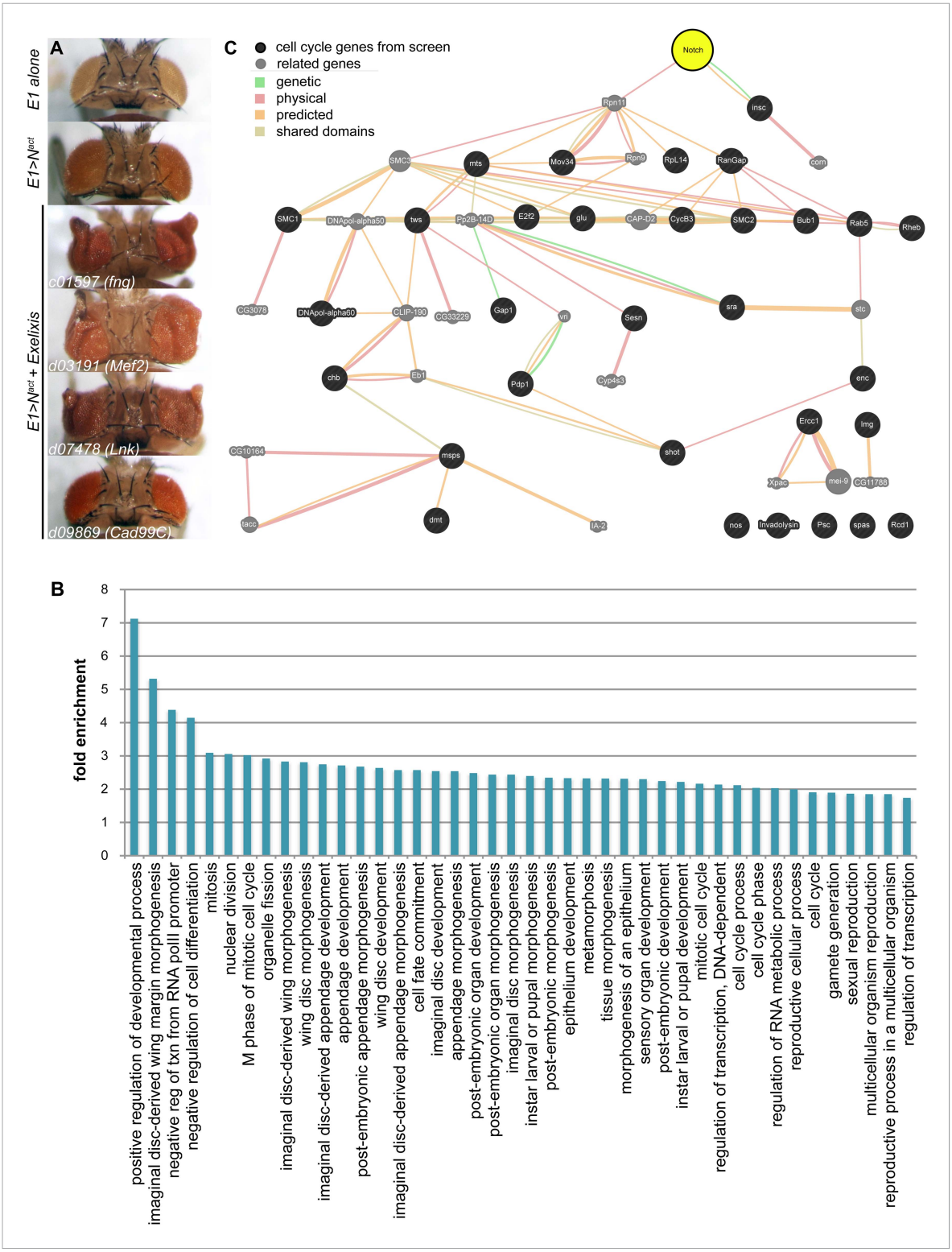

Figure 1. A genetic screen for modifiers of Notch-induced proliferation in the *Drosophila* eye. (**A**) Examples of screen phenotypes. *E1>N^{act}* results in larger eyes (second panel), compared to wild-type (*E1Gal4* alone) controls (top panel). Examples of three enhancers, *c01597* (fng), *c03191* (Mef2), and *d07478* (Lck), and one suppressor, *d09869* (Cad99C), are shown. (**B**) Analysis of enrichment of GO terms among the 360 *Drosophila* genes identified in the screen. Only enriched terms with corrected p-value < 0.05 (using Benjamini–Hochberg correction) are shown. For numerical p-values, please see ***Supplementary file 2***. (**C**) Gene association analysis among cell cycle genes identified in the genetic screen. Genetic interactions, physical interactions, predicted interactions, and shared protein domains were mapped using GeneMania (www.genemania.org) between the 31 cell cycle genes from our

Figure 1. continued on next page

Figure 1. Continued

screen (black circles) and Notch (yellow). Genes labeled with grey circles are part of the network but were not identified in our screen.
DOI: 10.7554/eLife.05996.003

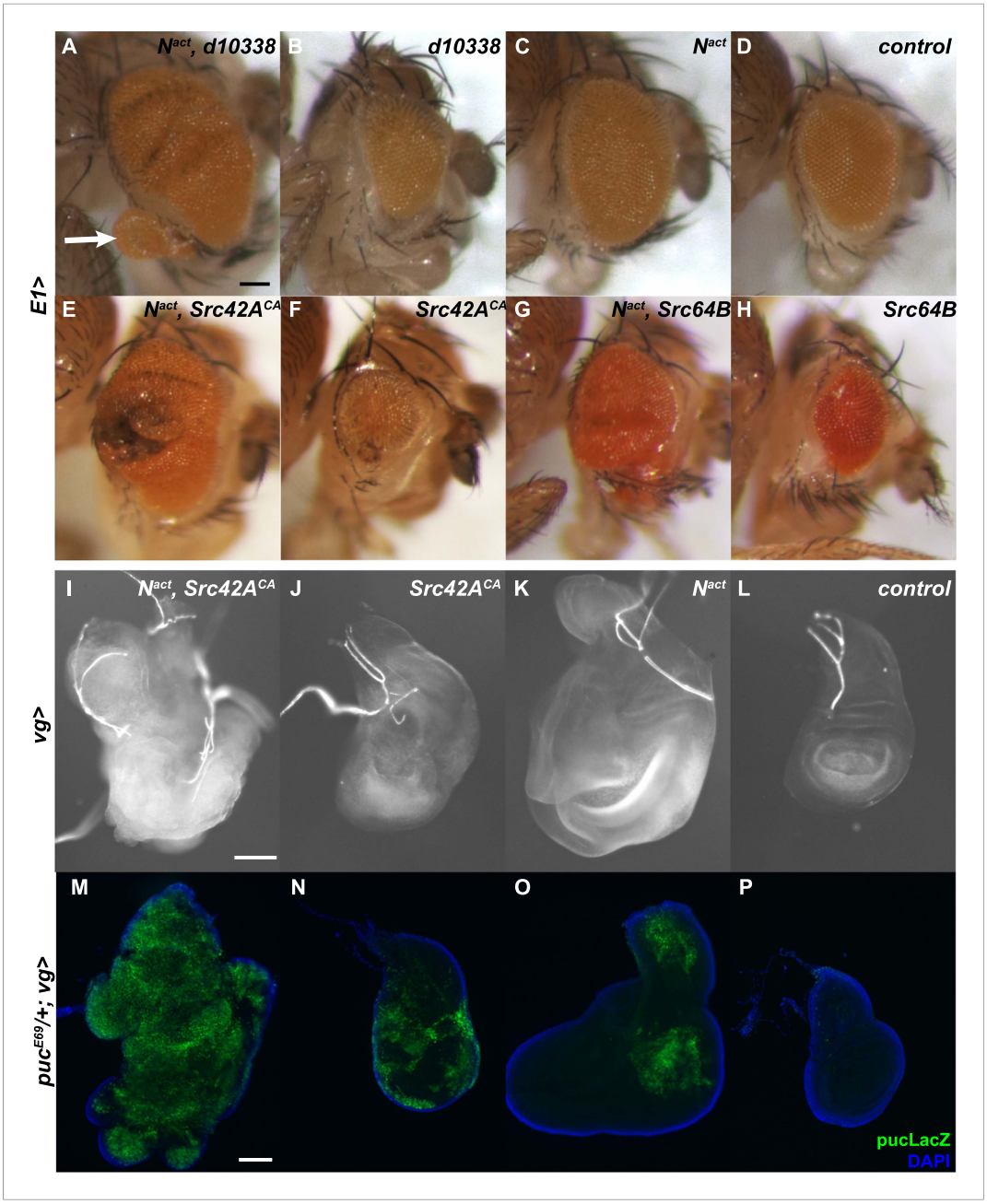

Figure 2. Synergy between Notch and Src in the eye and wing causes hyperplastic phenotypes and activates JNK. (**A**–**H**) Various *UAS-Src* constructs were driven by *E1Gal4* along with UAS-N^{act} in the developing eye. When *d10338*, an Exelixis allele that causes Gal4-dependent overexpression of Src42A, and N^{act} are coexpressed (**A**), the N^{act} large eye phenotype (**C**) is enhanced; in addition, occasional outgrowths of eye tissue can be seen (arrow). Note that d10338 alone (**B**) results in decreased eye size, whereas N^{act} alone (**C**) results in increased eye size compared to the control (**D**). Src42A^{CA} and Src64B both cause a similar phenotype (**E**, **G**) when coexpressed with N^{act} under *E1Gal4*, and both also result in decreased eye size in the absence of N^{act} (**F**, **H**). (**I**–**L**) *UAS-N^{act}* and *UAS-Src42A^{CA}* were driven in the developing wing using the *vgGal4* driver. When N^{act} and Src42A^{CA} are co-expressed (**I**), wing discs are overgrown compared to either Src42A^{CA} (**J**) or N^{act} (**K**) alone and display a characteristic 'crumpled ball' phenotype indicative of tissue disorganization and cell migration. Note that Src42A^{CA} alone (**J**) causes disorganization but not overgrowth. (**M**–**P**) *Puc-LacZ* reporter assay for JNK signal activation in wing discs expressing UAS constructs as indicated under the *vgGal4* driver in a *puc^{E69}*/+ background. Coexpression of N^{act} and Src42A^{CA} (**M**) causes strong, global activation of the *pucLacZ* reporter. In contrast, expression of either gene alone (**N**, **O**) causes weaker activation that is limited in scope. Scale bars: 100 μm.

DOI: 10.7554/eLife.05996.004

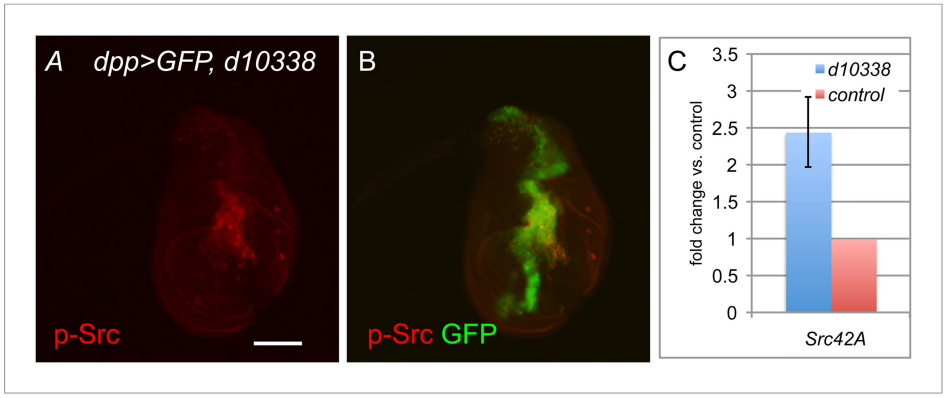

Figure 2—figure supplement 1. *d10338* is a UAS allele of *Src42A*. (**A**, **B**) *UAS-GFP/d10338; dppGal4/+* wing discs were stained for anti-phosphoY418-Src (p-Src, red), which labels activated Src. Scale bar: 100 μm. (**C**) qPCR for *Src42A* in *MS1096Gal4/+; d10338/+* wing discs (blue bar) or *MS1096Gal4/+* controls (red bar). Mean values are shown for two independent biological replicates.

DOI: 10.7554/eLife.05996.005

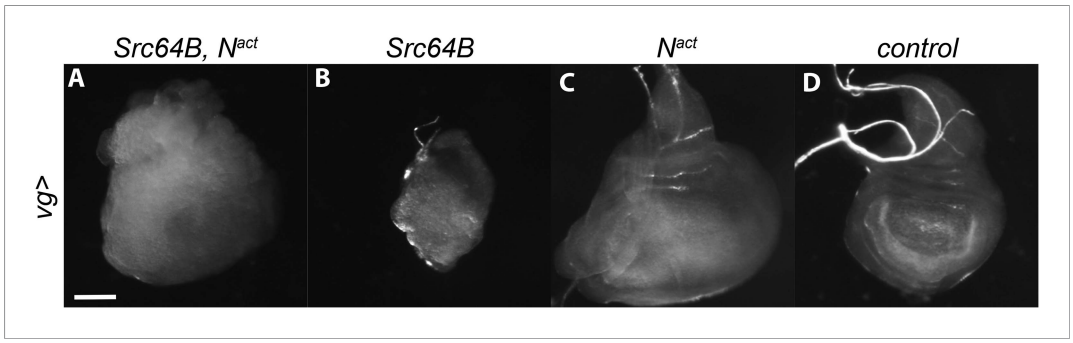

Figure 2—figure supplement 2. Src64B also synergizes with N^{act} in the wing disc. When driven with *vgGal4*, Src64B and N^{act} synergize to produce an overgrown, disorganized disc (**A**), whereas Src64B alone causes disorganization (**B**) and N^{act} alone causes large but organized discs (**C**) compared to control (**D**). Scale bar: 100 μm.

DOI: 10.7554/eLife.05996.006

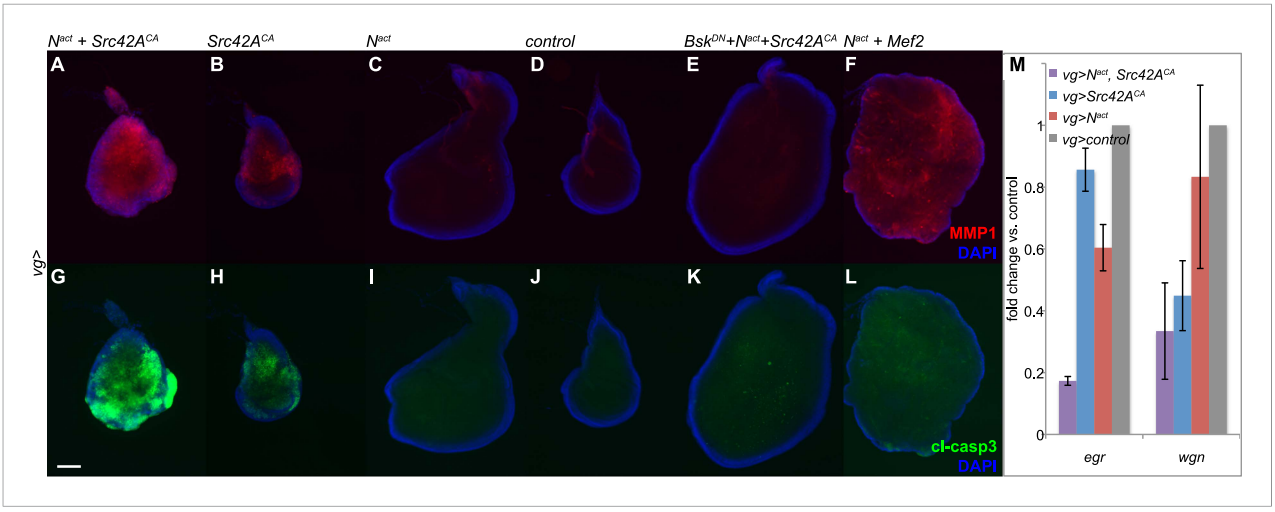

Figure 3. N/Src synergy induces both MMP1 and apoptosis. (**A**–**L**) Immunofluorescence for MMP1 (**A**–**F**) and cleaved caspase 3 (cl-casp3, **G**–**L**) in wing discs expressing UAS constructs under *vgGal4*. Together, N^{act} and $Src42A^{CA}$ cause robust activation of both MMP1 (**A**) and cl-casp3 (**G**), which is strongly reduced by Bsk^{DN} (**E**, **K**). The combination of N^{act} and Mef2 results in an increase in MMP1 (**F**) but little effect on cc3 (**L**). (**M**) qPCR for *egr* and *wgn* in wing discs overexpressing genes as indicated under the *vgGal4* driver reveals that both transcripts are strongly downregulated when N^{act} and $Src42A^{CA}$ are coexpressed. Scale bar: 100 μm.

DOI: 10.7554/eLife.05996.007

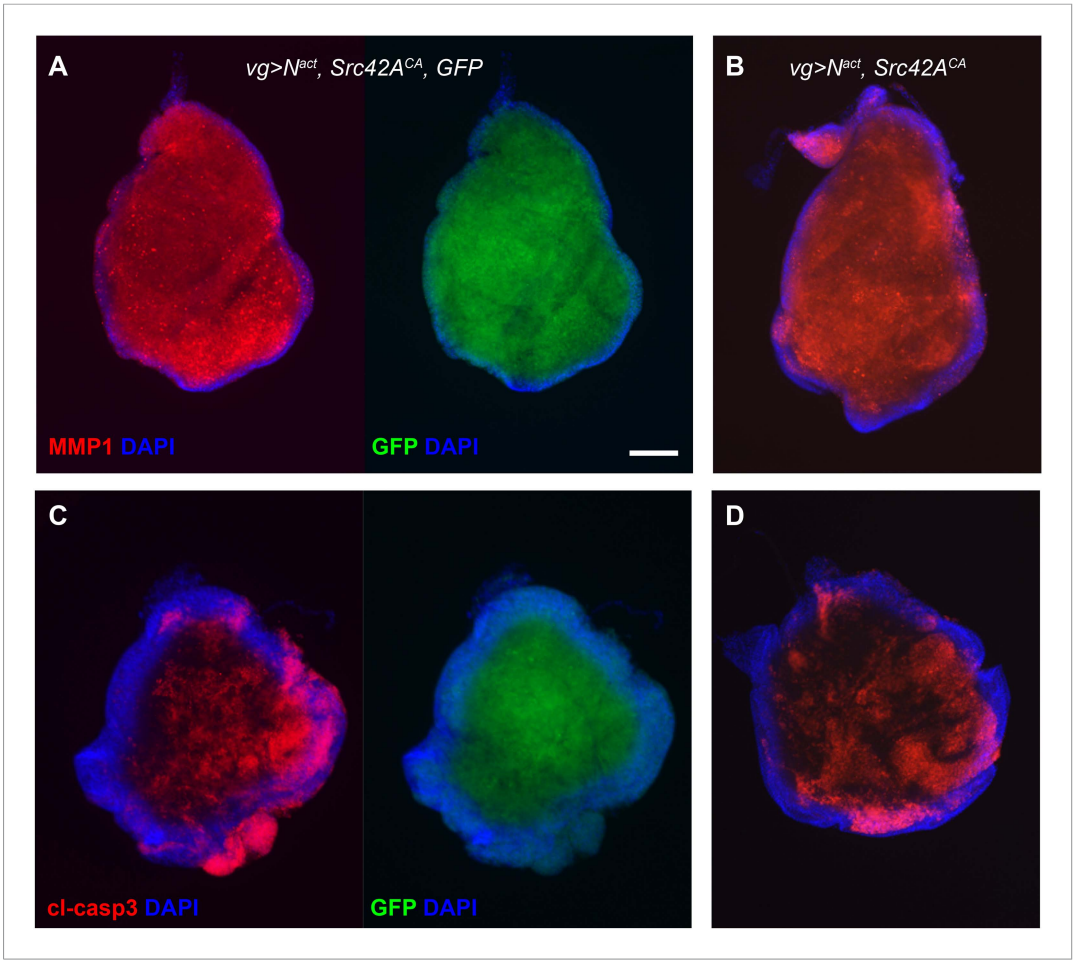

Figure 3—figure supplement 1. Gal4/UAS titration does not affect the N/Src phenotype. (**A**, **C**) One copy each of *UAS-N^{act}*, *UAS-Src42A^{CA}*, and *UAS-GFP* (three UAS transgenes total) were driven with *vgGal4* in the wing disc, and compared to (**B**, **D**) wing discs expressing only *UAS-N^{act}* and *UAS-Src42A^{CA}* (two UAS transgenes total) with *vgGal4*. Discs were stained for MMP1 (**A**, **B**) or cleaved caspase 3 (**C**, **D**). Scale bar: 100 μM.

DOI: 10.7554/eLife.05996.008

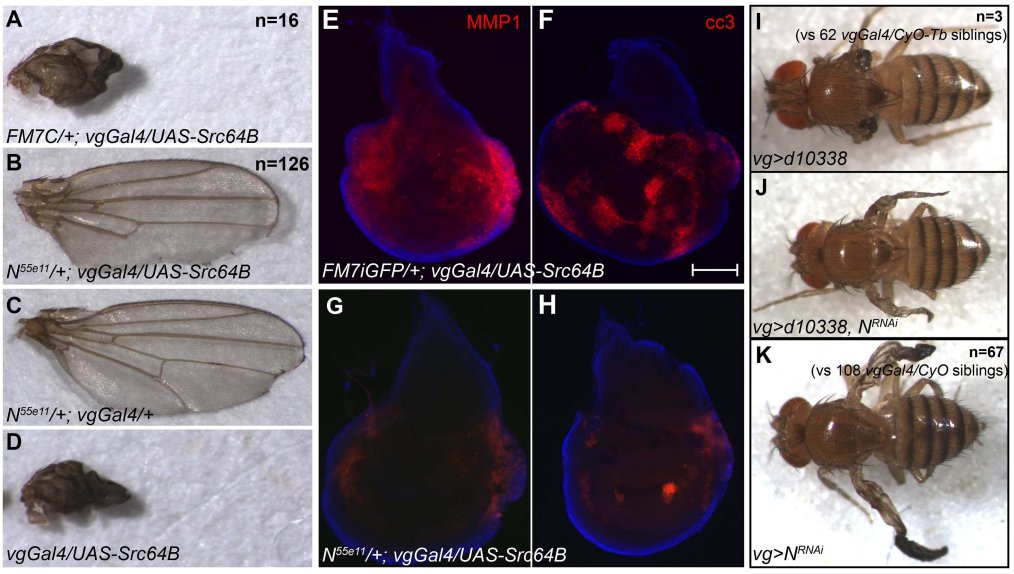

Figure 3—figure supplement 2. A heterozygous null mutation of Notch can rescue lethality and phenotype of Src alone. N^{55e11}/*FM7C;UAS-Src64B* virgins were crossed to *vgGal4* males at 18˚C (**A**, **B**) and the resultant female progeny were scored. N^{55e11}/+;*vgGal4/UAS-Src64B* flies were more viable (**B**, n = 126 over four independent experiments) than their *FM7C/+;vgGal4/UAS-Src64B* siblings (**A**, n = 16), and show a rescued phenotype similar to that of N^{55e11}/+;*vgGal4/+* controls (**C**). *FM7C/+;vgGal4/UAS-Src64B* (**A**) wings were indistinguishable from *vgGal4/UAS-Src64B* (**D**) wings. (**E**–**H**) Immunostaining for MMP1 (**E**, **G**) or cleaved caspase 3 (**F**, **H**) in wing discs with genotypes (**D**, **E**) *FM7iGFP/+;vgGal4/UAS-Src64B* or (**F**, **G**) N^{55e11}/+;*vgGal4/UAS-Src64B*. Scale bar: 100 μm. (**I**–**K**) *d10338* (Exelixis *Src42A* allele) lethality and phenotype at 25˚C can be partially rescued by Notch RNAi. *vgGal4/d10338* flies (**I**) are largely pupal lethal (n = 3 viable adults compared to 62 *vgGal4/CyO-Tb* siblings from the same cross) and the few escapers have no wings. In contrast, *vgGal4/d10338, UAS-*N^{RNAi} flies (**J**) have narrow, short, and shriveled wings and much lower lethality (n = 67, compared to 108 *vgGal4/CyO* siblings from the same cross.) The wing phenotype appears to be a more severe version of the phenotype of *vgGal4/UAS-*N^{RNAi} flies (**K**).

DOI: 10.7554/eLife.05996.009

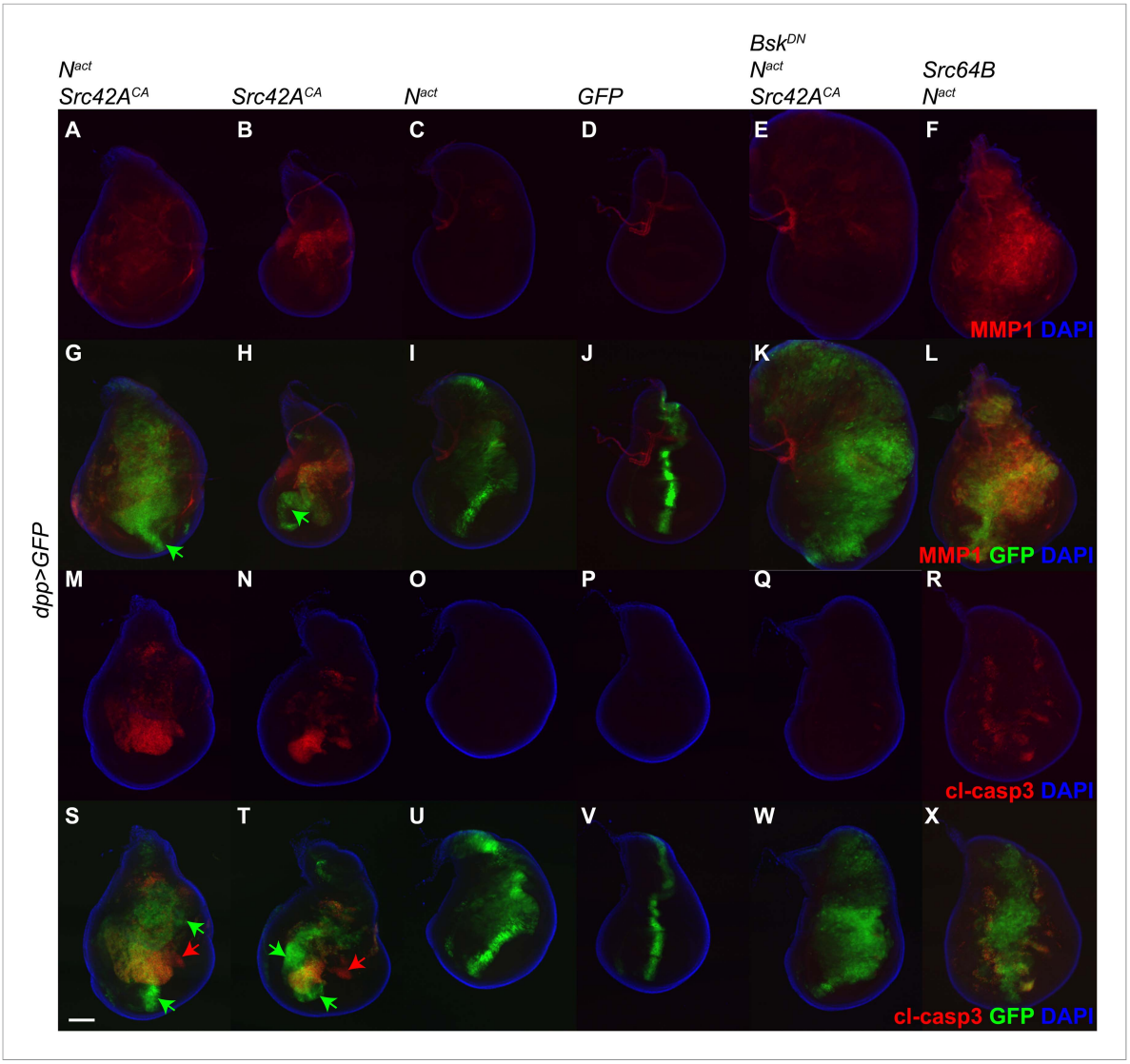

Figure 4. *dpp-Gal4* driven expression of N^{act} and $Src42A^{CA}$ also upregulates MMP1 and induces apoptosis. UAS transgenes as indicated were driven with *dppGal4* along with *UAS-GFP* at 18°C. Controls express an extra copy of *UAS-GFP*. Wing discs were stained with anti-MMP1 (**A**–**L**) or anti-cleaved caspase 3 (cl-casp3, **M**–**X**). The combination of N^{act} and $Src42A^{CA}$ induces both MMP1 (**A**, **G**) and cl-casp3 (**M**, **S**), and $Src42A^{CA}$ alone does the same to a lesser extent (**B**, **H**, **N**, **T**). Green arrows: GFP positive cells that do not express MMP1 (**G**, **H**) or cl-casp3 (**S**, **T**). Red arrows: cl-casp3-positive cells that do not express GFP, indicating a potentially non-cell-autonomous effect. This effect can be largely rescued with Bsk^{DN} (**E**, **K**, **Q**, **W**). Similarly, the combination of Src64B and N^{act} also induces both MMP1 (**F**, **L**) and cl-casp3 (**R**, **X**). Scale bar: 100 μM.

DOI: 10.7554/eLife.05996.010

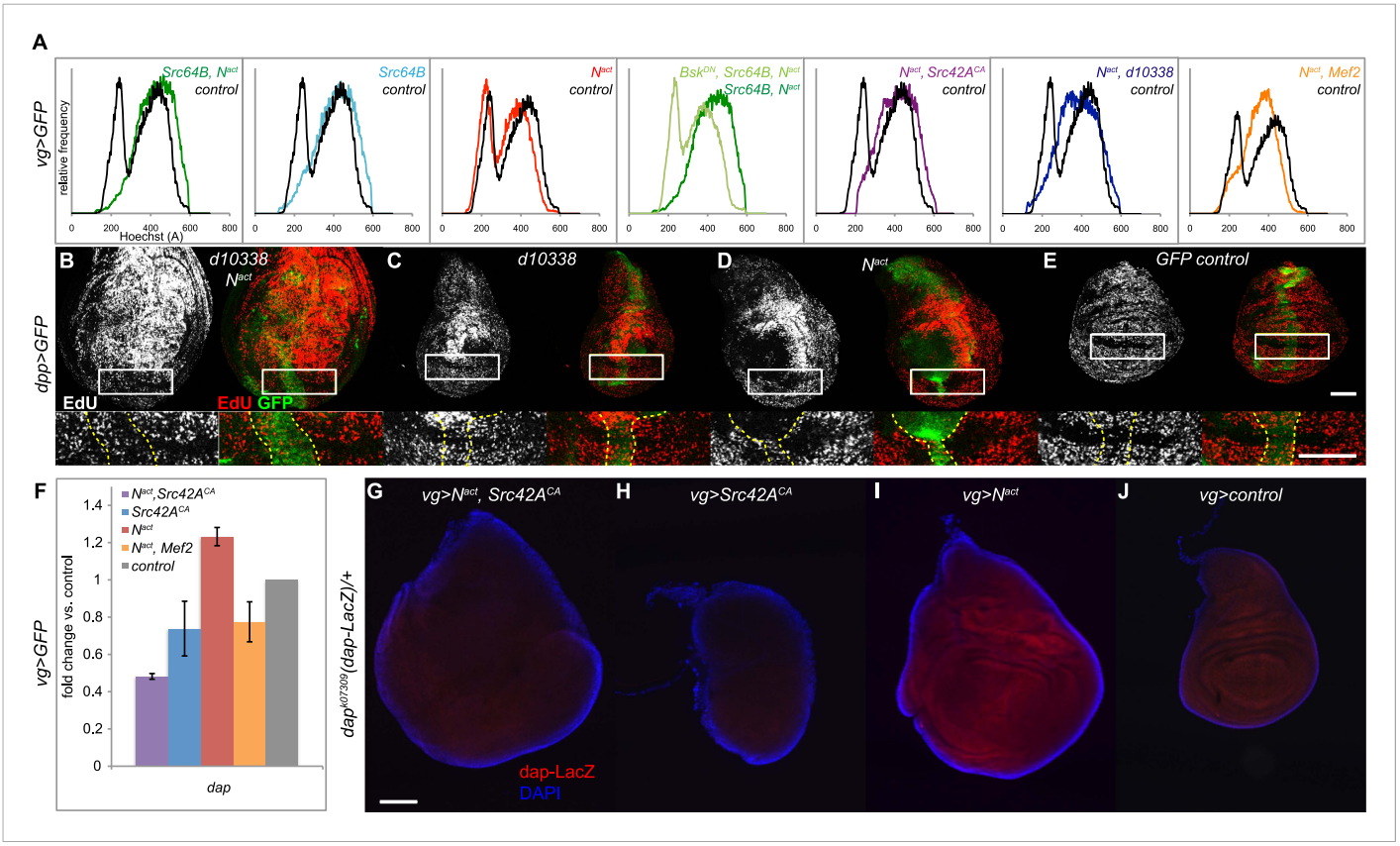

Figure 5. N/Src synergy disrupts the cell cycle. (**A**) DNA content analysis was performed on Hoechst-labeled dissociated cells from *vgGal4;UAS-GFP* wing discs expressing *UAS-Src64B;UAS-N^{act}* (dark green trace), *UAS-Src64B* (light blue), *UAS-N^{act}* (red), WT control (black), *UAS-Bsk^{DN};UAS-Src64B;UAS-N^{act}* (light green), *UAS-N^{act};UAS-Src42A^{CA}* (purple), *UAS-N^{act};d10338* (dark blue) or *UAS- N^{act};UAS-Mef2* (orange). Comparative histograms show relative frequencies on the y-axis, normalized to total number of counts for each sample. (**B**–**E**) EdU incorporation assay in *dppGal4;UAS-GFP* wing discs expressing *d10338;UAS-N^{act}* (**B**), *d10338* (**C**), *UAS-N^{act}* (**D**), or *UAS-GFP* (**E**) at 22˚C. A closeup of the areas denoted by boxes is shown below each image, and the GFP-positive area is marked with dotted yellow lines. Whereas *UAS-N^{act}* alone expands the ZNC (zone of non-proliferating cells) and also non-cell-autonomously induces proliferation in the dorsal-posterior region of the disc, thus increasing the size of the dorsal compartment (**D**), the combination of *d10338* and *UAS-N^{act}* eliminates the expansion of the non-proliferative zone and causes cells within the ZNC proper to begin incorporating EdU; furthermore, the area of increased proliferation in the dorsal compartment appears to be expanded (**B**). (**F**–**J**) N^{act} and Src42A^{CA} together cause a reduction in *dacapo (dap)* levels. (**F**) qPCR for *dap* expression in wing discs expressing N^{act} and/or Src42A^{CA} or Mef2 under the *vgGal4* driver. (**G**–**J**) A *dap-LacZ* reporter assay was used to visualize *dap* expression in *vgGal4* wing discs in a *dap^{k07309}*/+ background. Both N^{act} and Src42A^{CA} together (**G**) and Src42A^{CA} alone (**H**) show a reduction in dap-LacZ compared to both N^{act} alone (**I**) and *vgGal4* controls (**J**). Scale bars: 100 μM.

DOI: 10.7554/eLife.05996.011

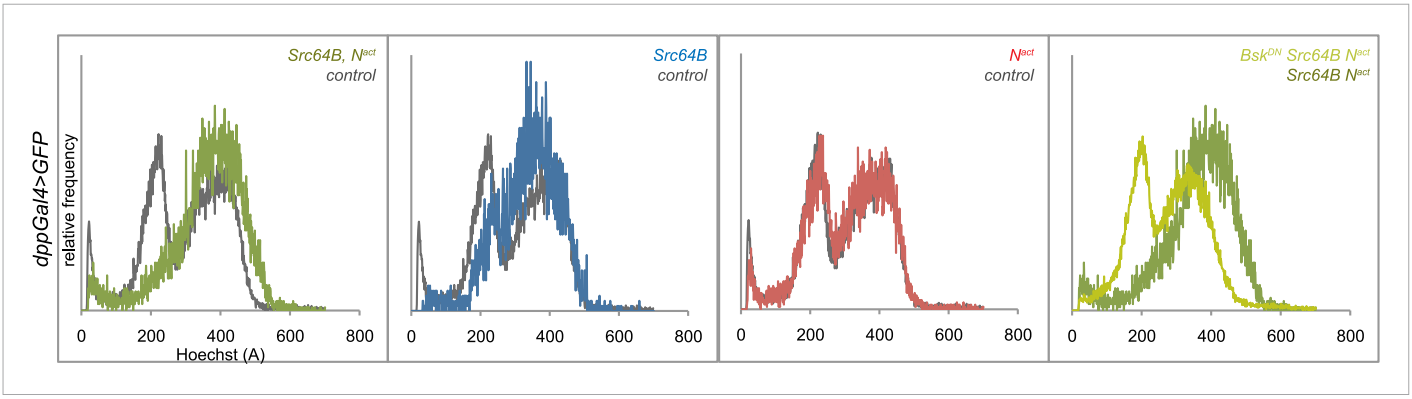

Figure 5—figure supplement 1. Elimination of G1 phase of the cell cycle also occurs in *dppGal4* wing discs expressing N^{act} and Src64B. DNA content analysis was performed on Hoechst-labeled dissociated cells from *dppGal4;UAS-GFP* wing discs expressing *UAS-Src64B;UAS-*N^{act} (green trace), *UAS-Src64B* (blue), *UAS-*N^{act} (red), WT control (grey), or *UAS-*Bsk^{DN}*;UAS-Src64B;UAS-* N^{act} (yellow-green). Comparative histograms show relative frequencies on the y-axis, normalized to total number of counts for each sample.

DOI: 10.7554/eLife.05996.012

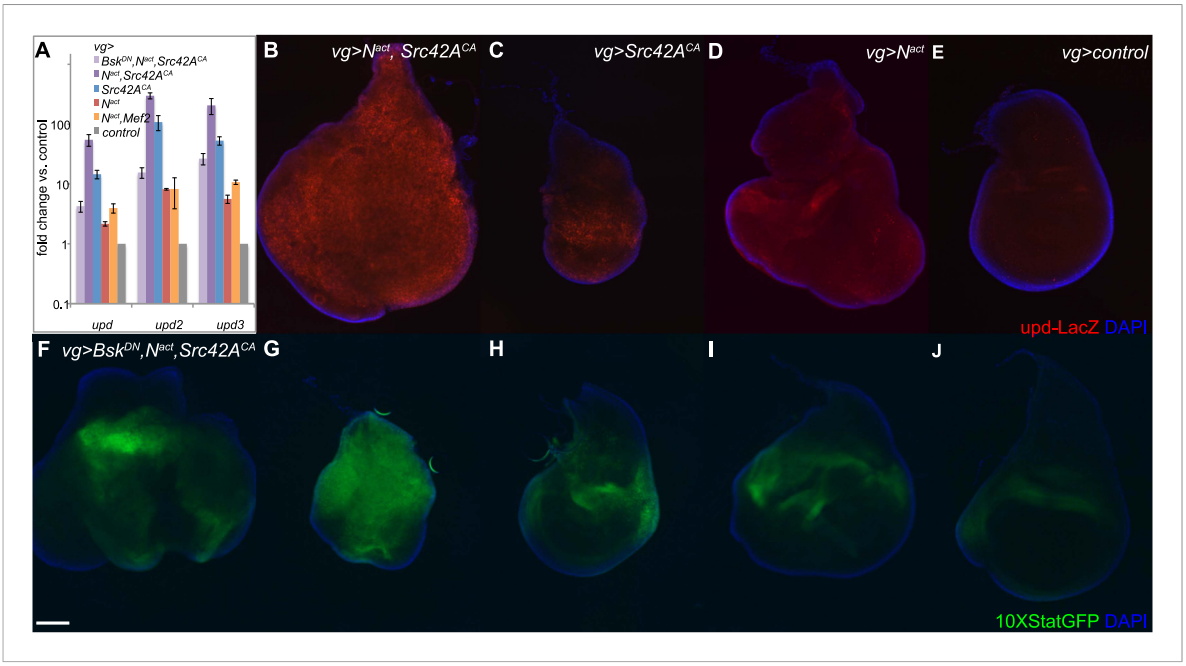

Figure 6. N/Src synergy activates the JAK/STAT signaling pathway. (**A**) qPCR for *unpaired* family ligands in *vgGal4* discs expressing UAS constructs as indicated. All three *upd* family genes are highly upregulated by the combination of N^{act} and $Src42A^{CA}$ (dark purple bars), and this upregulation is dependent upon JNK signaling as Bsk^{DN} rescues it (lavender bars). Coexpression of N^{act} and Mef2 (orange bars) induces a much lower level of the *upd* ligands. Note that the y-axis is on a logarithmic scale. (**B**–**E**) An *upd-LacZ* reporter assay in *vgGal4* wing discs validates the qPCR data and demonstrates that N^{act}+$Src42A^{CA}$ causes strong, widespread activation of *upd* transcription (**B**); in contrast, either gene alone (**C**, **D**) causes lower, more restricted levels of *upd* upregulation. (**F**–**J**) The *10XStatGFP* reporter was used to assess JAK/STAT signal activation in *vgGal4* discs grown at 18˚C. N^{act}+$Src42A^{CA}$ strongly upregulates *10XStatGFP* (**G**), whereas either gene alone (**H**, **I**) only weakly upregulates the reporter. The addition of Bsk^{DN} (**F**) reduces the *10XStatGFP* induced by N^{act}+$Src42A^{CA}$ (**G**) to levels similar to those of N^{act} alone (**I**). Note that since the *upd-LacZ* discs were grown at 25˚C and the *10XSTATGFP* discs were grown at 18˚C, the latter displays a somewhat weaker phenotype, hence the difference in disc size between **B**/**D** and **G**/**I**. Scale bar: 100 μm.

DOI: 10.7554/eLife.05996.013

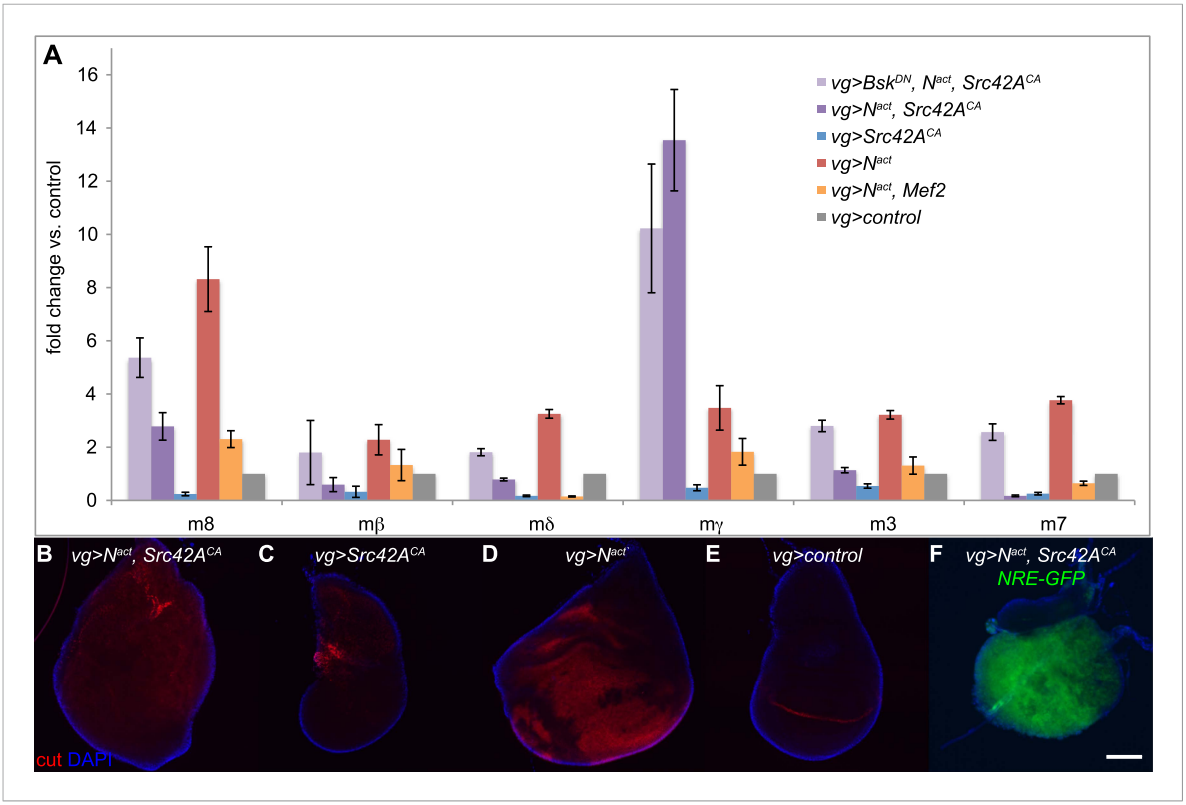

Figure 7. Notch targets are differentially affected by N/Src synergy. (**A**) qPCR assay for expression levels of *E(spl)* complex members in *vgGal4* wing discs expressing UAS constructs as indicated. (**B**–**E**) Immunostaining with anti-cut (red) in *vgGal4* wing discs. N^{act} alone (**D**) induces cut expression, which is suppressed in N^{act}+$Src42A^{CA}$ discs (**B**). Note that both ectopic and endogenous cut appear to be suppressed. (**F**) NRE-GFP expression in wing discs expressing N^{act}+$Src42A^{CA}$ under *vgGal4*. Scale bar: 100 μm.

DOI: 10.7554/eLife.05996.014

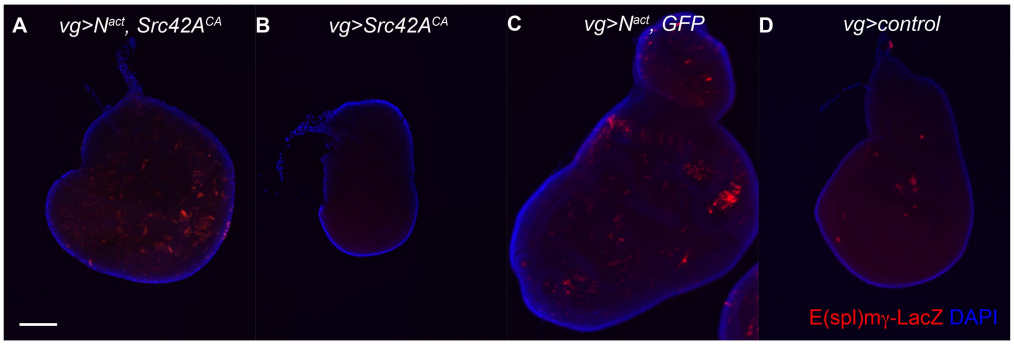

Figure 7—figure supplement 1. E(spl)mγ reporter staining in N/Src wing discs. *VgGal4* wing discs expressing *UAS-*N^{act} and/or *UAS-*$Src42A^{CA}$ in an *E(spl)mγ-LacZ*/+ background were stained for anti-β-gal. *E(spl)mγ-LacZ* consists of the 234-bp *mγ* enhancer region fused to a LacZ reporter (***Nellesen et al., 1999***). Note that E(spl)mγ induced by N^{act} (**C**) is not suppressed by the addition of $Src42A^{CA}$ (**A**). $Src42A^{CA}$ alone (**B**) seems to suppress the endogenous E(spl) mγ staining (**D**) in the proneural cells.

DOI: 10.7554/eLife.05996.015

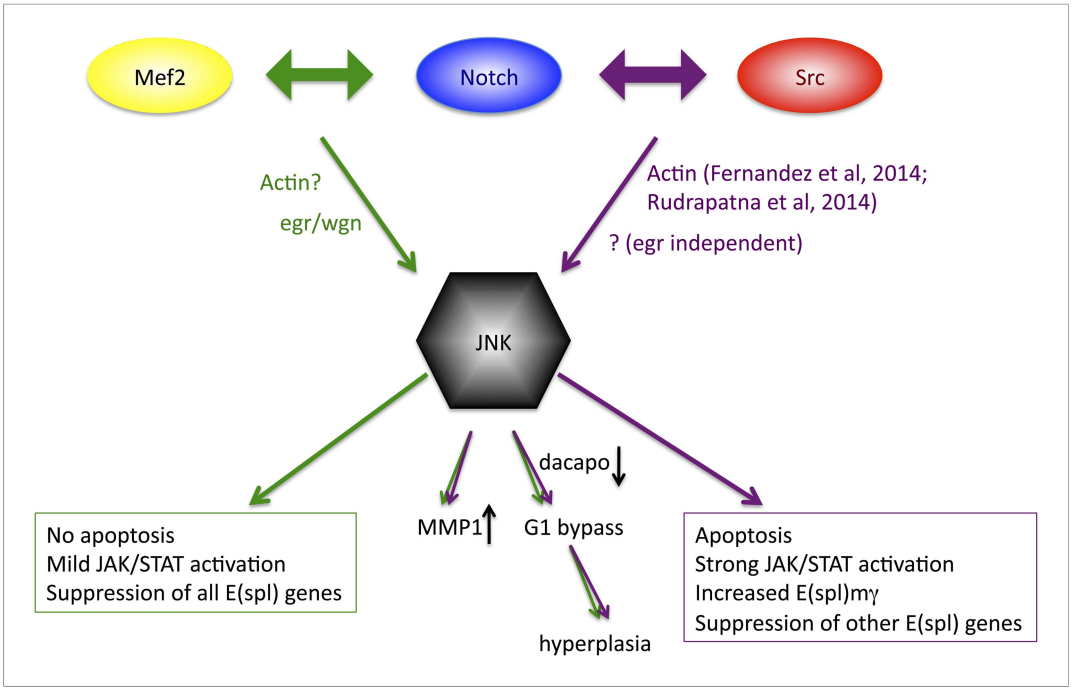

Figure 8. Model of convergence and divergence of the Notch/Mef2/JNK and Notch/Src/JNK signaling axes. N/Mef2 and N/Src synergies converge on JNK, through *eiger*-dependent and *eiger*-independent means respectively. Some downstream processes are common to both synergies, such as MMP1 activation and bypass of G1 phase of the cell cycle via *dap* downregulation. Other downstream outputs, such as apoptosis, level of JAK/STAT activation, and regulation of Notch target genes, diverge between N/Src and N/Mef2 synergy.

DOI: 10.7554/eLife.05996.016